Feedback Control of CSD in a KCl Crystallizer with a Fines Dissolver

On-line crystal size distribution control in an 18 L KCl crystallizer, equipped with a fines dissolver, was experimentally studied using inferential control of nuclei density. The control algorithm used was proportional control of inferred nuclei density by manipulation of fines removal rate. A sudden 5-8°C drop in the temperature of the crystallizer was used as a standard upset, which produced a fairly reproducible burst of nuclei. Nuclei density was then estimated from the fine crystal distribution in the fines loop using a light-scattering instrument. The control study was implemented by a computer program that used the current value of nuclei density to calculate updated set points of the fines removal rate. Simple proportional control of nuclei density in response to changes in fines removal rate was shown to be an effective way to minimize fluctuations in the product crystal size distribution that are caused by nucleation disturbances.

A. D. Randolph, Li Chen, and Aria Tavana
Department of Chemical Engineering
University of Arizona
Tucson, AZ 85721

Introduction

Crystal size distribution (CSD) is one of the most important properties of a crystallization process; it often determines final purity, based on dewatering ease, as well as handling and many end use properties. Little work has been done in the area of experimental feedback control of CSD, although there have been several theoretical and numerical studies reported. These studies include work by Beckman and Randolph (1977), Epstein and Sowul (1980), Gupta and Timm (1971), Johnson et al. (1985), Lei et al. (1971), and Rousseau and Howell (1982). The lack of experimental CSD control studies is probably due to the previous lack of convenient on-line techniques for particle size analysis. Currently available light-scattering instruments have made possible on-line measurement of fine-crystal populations which may yield enough information to permit on-line CSD control.

The purpose of this paper is to describe an experimental study of inferential on-line CSD control recently suggested (U.S. Patent, 1981). The system used was a KCl crystallizer equipped with a fines dissolver. The control algorithm used the inferential estimation of nuclei population density n^0 from light-scattering measurements in a continuous fines stream. The value of n^0 was then controlled by manipulation of a fines dissolving stream.

Previous Work

Recent studies (Randolph et al., 1981; Rovang and Randolph, 1980) have developed the technology for on-line estimation of crystallization properties, e.g., nucleation rate B^0, and growth rate G, from fine-crystal populations. Manipulation of both fines dissolver flow rate and dissolver temperature in response to changes in estimated nuclei density has been used in an attempt to control CSD in a KCl crystallizer (Randolph and Low, 1982). Manipulation of fines dissolver rate apparently upset fine crystal removal in the fines classifier and did not show effective CSD control. However, partial dissolution of fines, obtained by manipulation of dissolver temperature, did appear to reduce the transient effects on CSD of imposed upsets in nucleation rate. Neither partial fines dissolving nor manipulation of fines removal rate gave a linear response of nuclei destruction to the change in manipulated variable. In spite of numerous theoretical studies of CSD control, the work of Randolph and Low (1982) is the only reported experimental study of direct feedback control of CSD.

In the present study a linear response of nuclei removal was maintained by keeping fines removal constant. The manipulated variable was then the fraction of fines recycled back to the crystallizer.

Theoretical Considerations

There are two types of dynamic modes that a crystallizer experiences, CSD instability and CSD transients. Instability is

The current address of Li Chen is Tienjin University, Tienjin, China.

caused by the interaction of system kinetics and process configuration, whereas transients are caused by outside disturbances, e.g., changes in flow rates, temperature, or agitation. Beckman and Randolph (1977) presented a theoretical study of CSD instability in which it was shown that an unstable CSD could be stabilized by simple proportion control of nuclei density. In the present study we only considered control of CSD transients since our crystallizer was intrinsically stable. The current value of nuclei density, n^0, was estimated from on-line fines measurement and control was attempted by manipulating the fraction of the fines dissolver flow rate actually sent to the dissolver, Q_F. The proportional control algorithm used was simply given as

$$\left(\frac{Q_F - \bar{Q}_F}{\bar{Q}_F}\right) = K_c\left(\frac{n^0 - \bar{n}^0}{\bar{n}^0}\right) \tag{1}$$

where steady state variables are indicated by the overbar. The choice of n^0 as an inferential control variable was made because many types of upsets influence nucleation rate and hence nuclei density. Further, at constant slurry density a constant value of n^0 is necessary to maintain CSD constant. Finally, nuclei density can be inferred on-line by process-feasible light-scattering instruments applied to a conditioned fines stream. Fines dissolving rate was chosen as the manipulated variable since fines removal is the most direct method of influencing nuclei population density. The dimensionless gain K_c was set at 0.5 based on a previous theoretical control study (Beckman and Randolph, 1977).

A root mean square (RMS) measure of CSD fluctuations was used as a performance index to evaluate control. Thus,

$$(PI)^2 = \frac{1}{N}\sum_{i=1}^{N}\left(\frac{\Delta W_i - \overline{\Delta W_i}}{\overline{\Delta W_i}}\right)^2 \tag{2}$$

where ΔW_i is the weight fraction of crystal product in sieve range i and N is the number of samples. CSD data were also converted to particle number density, and plotted as a function of time to directly observe the control of crystal population. The population density was calculated from the weight fraction by the following equation:

$$n(L) = \frac{M_T \Delta W(L)}{\rho k_v \bar{L}^3 \Delta L} \tag{3}$$

where M_T refers to slurry density in the crystallizer (grams of solid per liter of clear liquid) and k_v is the shape factor converting size cubed to particle volume.

The steady state solution of the population density function for an mixed-suspension, mixed-product removal (MSMPR) crystallizer is given as:

$$n(L) = n^0 \exp\left(\frac{-L}{G\tau}\right) \tag{4}$$

Equation 4 also holds for the mixed-removal fines distribution up to classification size L_F, where τ is now the mean retention time of the fines, $\tau_F = V/(Q_F + Q_i)$. If the fines distribution is essentially of exponential form, i.e., the majority of the numbers in the distribution are given by Eq. 4, then a simple technique for estimating nuclei density n^0 is shown as follows.

The mass density of the fines distribution is given as:

$$M_{T_F} = \rho k_v \int_o^\infty nL^3\, dL \tag{5}$$

Bringing Eq. 4 to Eq. 5 and integrating gives the fines slurry density as:

$$M_{T_F} = 6\rho k_v n^0 (G\tau_F)^4 \tag{6}$$

The mass-weighted average size for the fines distribution is given as:

$$(\bar{L}_{4,3})_F = 4(G\tau)_F \equiv \sum L_i \Delta W_{i_F} \Big/ \sum_i \Delta W_{i_F} \tag{7}$$

Bringing Eq. 7 to Eq. 6 and solving for n^0 yields:

$$n^0 = 4^4 M_{T_F}/6\rho k_v (\bar{L}_{4,3})_F^4 \tag{8}$$

Nuclei density was estimated directly from Eq. 8. It is noted that Eq. 8 represents an integral, rather than a differential, technique for calculating nuclei density. A standard differential technique would be to graph $n \equiv \Delta N/\Delta L$ on a semilog plot and extrapolate to $L = 0$ to obtain n^0 as the intercept (Beckman and Randolph, 1977; Randolph and Low, 1982).

Experimental Apparatus and Technique

The apparatus used was the same KCl crystallizer that has been described previously (Randolph and Low, 1982). Fines CSD measurement and data reduction were obtained on a Cilas Granulometer 715 light-scattering particle analyzer in connection with a Hewlett Packard 85 minicomputer.

The KCl crystallizer consists of a well-mixed, draft-tube-baffled crytallizer as described in Table 3, with an associated fines dissolution system, as diagramed in Figure 1. The crystallizer is 0.31 m in diameter and 0.42 m long, with a working volume of 18×10^{-3} m^3. Two stainless steel cooling coils are arranged concentrically within the crystallizer: a 10.2 cm (4 in.) dia. coil of 1.3 cm (½ in.) tubing, and a 20.3 cm (8 in.) dia. coil of 0.95 cm (⅜ in.) tubing. Three vertical baffles attached to the coils rest against the tank walls. Three other baffles divide the annulus between the coils. The impeller, located within the inner coil, is a three-blade marine-type propeller of 3.7×10^{-2} m radius.

Saturated KCl solution at 54°C was fed from a 200 L (0.2 m^3) feed tank. A double draw-off product removal system was used, giving crystal product residence times of 180–240 min, depending on the ratio of overflow to underflow streams. Suspension densities ranged from $(30–120) \times 10^{-3}$ kg of crystals per liter of clear liquor. The fines stream was removed from an internal fines trap that classified the crystals with a cut size of about 180×10^{-6} m. A separate fines classifier having a cut size adjustable between $(100–200) \times 10^{-6}$ m was used to condition the sample stream continuously flowing through the sample cell of the Cilas particle-sizing instrument (the maximum crystal size detected by the instrument was 192×10^{-6} m). The sample window was a rectangular slit about 25 mm × 25 mm (2 in. × 2 in.), having a flow thickness of 1 mm. No plugging of this sample window was observed due to particles in the sample stream. However, the sample window was flushed on a two-hour basis with the dissolved fines stream to prevent salt encrustation.

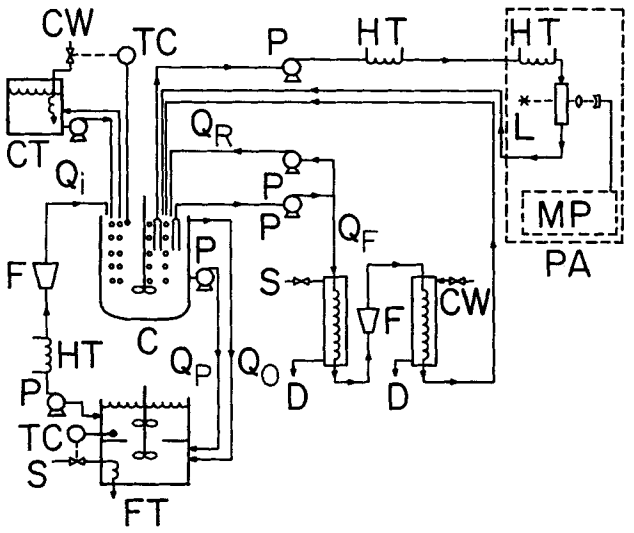

Figure 1. Flow diagram of 18 L crystallizer.

Crystal dissolution was achieved by raising the fines stream temperature to 54–60°C. This fines stream was then cooled and returned to the crystallizer. The system was assumed to be at steady state when the changes in ΔW_i with time for each sieve were minimal.

The crystallizer was first brought to steady state and then challenged with a sudden nucleation pulse obtained by upsetting the temperature. The temperature was upset by shutting off the cooling water until the temperature was raised by the incoming feed brine by the desired amount (~5–8°C). The cooling water was then opened to initiate temperature control. The sudden drop in the crystallizer temperature resulted in a fairly reproducible burst of nuclei. The CSD was measured throughout the experiment, on an hourly basis, by sieve analysis as well as by on-line measurement of n^0. Each run was 30–50 h in length. The control study was implemented by a program on the computer (HP-85), which used the current value of $\bar{n}^0$ to calculate updated setpoints of Q_F for the next sample period, as per Eq. 1. A three-point running time average of n^0 was used in the control algorithm. Thus,

$$\bar{n}_t^0 = (\bar{n}_{t-2}^0 + 2\bar{n}_{t-1} + n_t^0)/4 \tag{9}$$

where the overbar represents the time average and $()_t$ represents the value at sample period t. A sampled data time of 10 min was used, which permitted manual adjustment of the fines dissolver flow Q_F. A sampled data time as low as 1 min would be possible with the system if Q_F were adjusted automatically. The sampled data time of 10 min was still short compared to the product residence time τ_p = 180–240 min. An important aspect of the experimental apparatus was that the fines dissolver stream was adjusted by recycle of a portion directly back to the crystallizer. The purpose of this recycle was to vary Q_F without changing the cut size of the fines being removed from the crystallizer. Figure 2 shows the variation of $\bar{n}_t^0$ with time as calculated by the minicomputer. The value of $\bar{n}_t^0$ was then used to calculate the next value of the controlled dissolver rate Q_F.

The nuclei density, given by Eq. 8, is a function of both the fines slurry density and the average particle size:

$$n^0 \propto \frac{M_{T_F}}{(\bar{L}_{4,3})_F^4} \tag{10}$$

It was expected that both $(\bar{L}_{4,3})_F$ and M_{T_F} would change significantly after a nucleation upset. To observe these changes, varia-

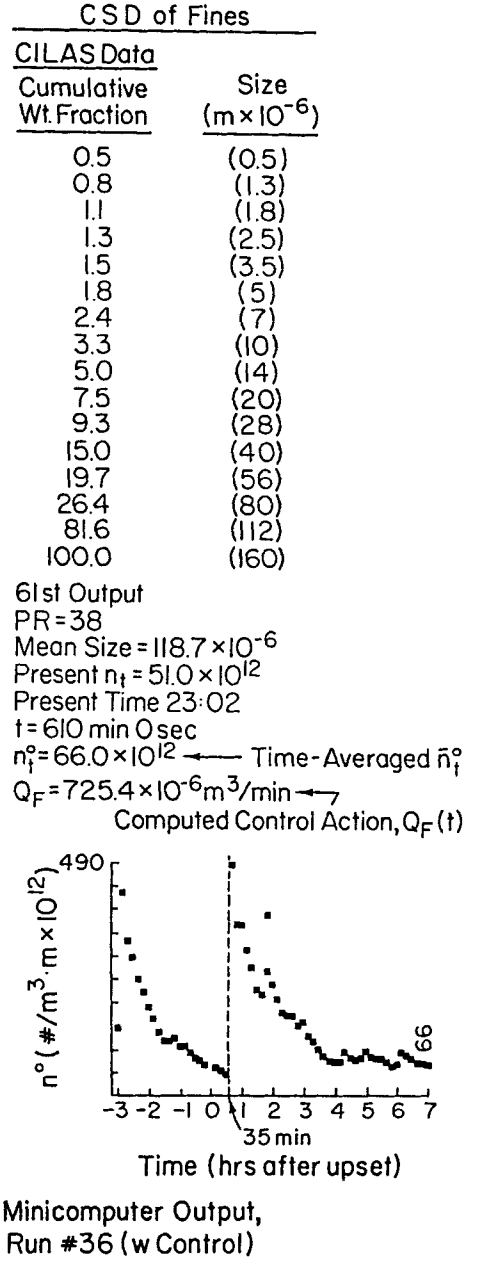

Figure 2. Representative computer output: time-averaged nuclei density vs. time.

tions of the average particle size and the slurry density of fines passing through the particle analyzer were followed with time. Figure 3 shows the variations of $(\bar{L}_{4,3})_F$ and M_{T_F} with time before and after a typical nucleation upset (run 36). It can be seen that aside from random fluctuations in the value of $(\bar{L}_{4,3})_F$ that occur throughout a run, there was no recognizable disturbance in $(\bar{L}_{4,3})_F$ due to the nucleation upset. For fines slurry density, on the other hand, there was a dramatic change. (It is not known if the outlying point shown at $t = 3$ h was real or was an artifact of the counter/printer system. This outlier is also evident in Figure 2). Following the upset in the temperature of the crystallizer, there is a decrease in M_{T_F} followed by a sudden jump in its value. It is apparent that the fines slurry density, not the fines linear size, drives the value of nuclei density. In other words,

$$n^0 \propto M_{T_F} \tag{11}$$

The large changes in M_{T_F} vis-a-vis $(\bar{L}_{4,3})_F$ appear to be real. (The computed fines histograms for runs 36 and 33 are discussed in detail in the Appendix.) The inferential n^0 control study discussed in this paper could have been done with a simpler instrument measuring only total suspended solids concentration of the fines.

To demonstrate that comparable control actions would have ben taken with or without measurement of the fines CSD, nuclei density was calculated as a function of time using two different methods. In the first method nuclei density was directly calculated from Eq. 8. In the second method an average value of $(\bar{L}_{4,3})_F$ (designated $\bar{\bar{L}}_{4,3})_F$ was inserted into Eq. 8 as a constant. The two estimates of n^0 thus calculated are compared in Figure 4. Values of nuclei density obtained by the two methods track each other closely except at the nuclei density peak. (The data

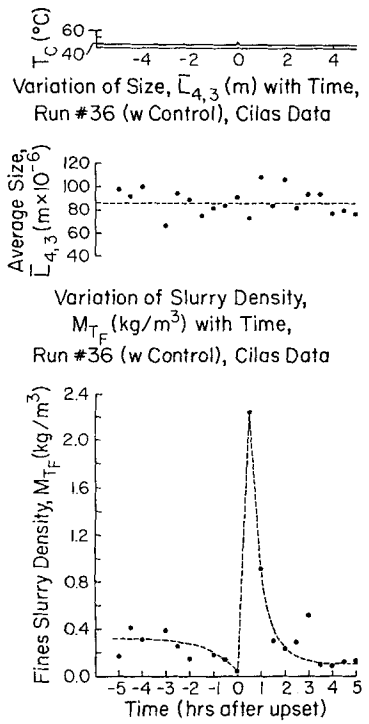

Figure 3. Variations of average particle size and fines slurry density due to a temperature upset.

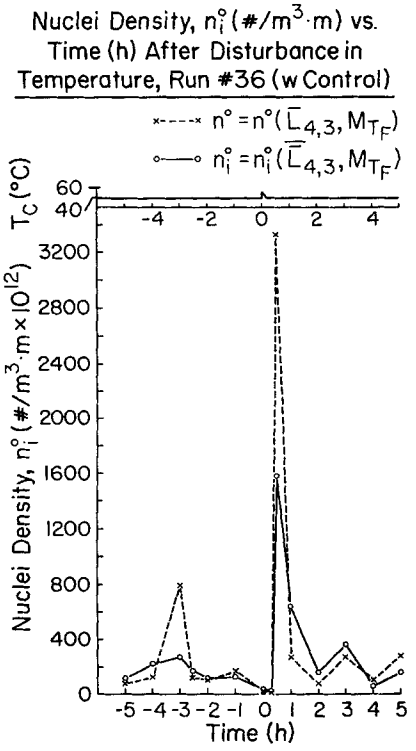

Figure 4. Nuclei density vs. time as a function of size and slurry density, and as a function of slurry density only.

point at $t = -3$ h can be neglected. At that time the values of $(\bar{L}_{4,3})_F$ dropped, due to plugging in the sampling system flow lines). Note that at the disturbance peak, the nuclei density, obtained by assuming $n^0 \propto M_{T_F}$, is sufficient to saturate the controller. For the given gain used, a fines destruction flow rate Q_F greater than 2,000 mL/min (0.002 m^3/min) was calculated, corresponding to saturation of the control action. Therefore, the assumption $n^0 \propto M_{T_F}$ would have resulted in essentially identical control actions. A total suspended solids fines slurry density sensor would have been sufficient for estimation of nuclei density, using Eq. 11.

Results

The performance index was evaluated for three runs: one with and two without feedback control. For each run a value of PI_1 was calculated for the steady state region before the temperature upset as well as a value after the upset, PI_2. PI_2 was calculated starting immediately after the nucleation upset and continuing until termination of the run. Termination of a run occurred when the disturbance had grown through the largest screen size or when operator fatigue or equipment failure mandated shutdown. The same average values $\Delta\bar{W}_i$ were used for PI_2 as for PI_1 since $\Delta\bar{W}_i$ refers to the average value of ΔW_i in the steady state region. The PI_1 and PI_2 values for runs 35 and 37 are averages of the two runs, averaged for each size range. The fluctuation in CSD caused by the temperature upset can be evaluated by comparing the PI_1 and PI_2 values for the two regions. Table 1 shows values of PI_1 and PI_2 with and without feedback control. There was a marked decrease in PI_2 values in run 36 when feedback control was implemented.

Table 1. Performance Index from Runs with and without Control

Size, m × 10^{-6}	Average for Runs 35 and 37*		Run 36**	
	$(PI_1)_{avg}$ %	$(PI_2)_{avg}$ %	PI_1 %	PI_2 %
1,000	19.1	68.7	21.3	41.9
841	7.5	62.1	4.5	23.1
707	9.3	37.3	5.2	6.3
595	7.1	90.6	5.4	26.5
500	7.7	158.2	8.6	46.6
↓500	14.9	248.2	10.0	78.8

*No feedback control.
**Feedback control.

Table 2. Ratio of Performance Indices with and without CSD Control

Size, m × 10^{-6}	$R_i = \frac{PI_2 \text{ without Control}}{PI_2 \text{ with Control}}$
1,000	1.6
841	2.7
707	5.9
595	3.4
500	3.4
↓500	3.2

$\bar{R} = \Sigma_i \Delta \bar{W}_i R_i = 3.45$.

Several other runs were attempted in addition to the three completed runs compared in Table 1. These runs are described as follows. Run 33 was intended as a run without control implementation. However, the run was stopped due to mechanical failure three hours after the temperature disturbance to the crystallizer. This amount of time was not sufficient for observing the effect of the nucleation pulse in large size ranges (>300 × 10^{-6} m). Therefore, data obtained from this run were not used for calculation of performance indices. In run 34 the nucleation upset failed. The operating conditions and the nature of the temperature upset were similar to other runs, but no noticeable disturbance in the population density or the weight fraction of particles was observed. Consequently, the data from this run were discarded. A possible explanation is that extraneous flushing water, used routinely to keep lines open, was added to the crystallizer. A second run with feedback control was attempted but failed mid-run due to pump failure.

The values of PI_2 for runs with no CSD control can be compared to PI_2 values with control as a ratio given by Eq. 12.

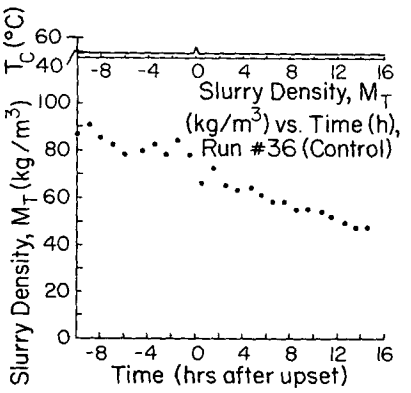

Figure 5. Reduction in slurry density with time.

Thus

$$R_i = \frac{PI_2 \text{ without control}}{PI_2 \text{ with control}} \tag{12}$$

where PI_2 again refers to the period following the nucleation upset. This ratio gives an idea of how well the control system has performed. Note that R_i is for a given size range ΔL_i with weight fraction ΔW_i. A mass-weighted average value $\bar{R}$ is given by Eq. 13.

$$\bar{R} = \sum_i R_i \Delta \bar{W}_i \tag{13}$$

Table 2 shows values R_i for the average of runs with and without control as well as the total mass-averaged performance index ratio for all runs. The application of feedback control significantly reduced mass-weighted PI_2 values by approximately a factor of 3.5 compared to runs without control.

A gradual reduction in slurry density was observed in all runs, Figure 5. This was due to fouling on the cooling coil. The slurry density for run 35 was markedly less than the other runs because the ratio of Q_o/Q_u for this run was set at 2 rather than 3. This change was made to possibly reduce the time it would take the crystallizer to reach steady state. However, no significant change in this time period was observed and the remaining runs were made at $Q_o/Q_u = 3$. Table 3 lists the range of variables used in this study.

The performance index ratio R is a quantitative measure of CSD controller performance. However, a better way to visualize the effect of CSD control is to follow the progression of the

Table 3. Range of Variables and Crystallizer Specifications

Run No.	Feed* m^3/min × 10^{-6}	Q_o/Q_u	Q_F m^3/min × 10^{-6}	RPM	Temperature, °C: Feed	Crystall.	Fines Destruction Loops	Crystall. Temp. Rise During Upset °C
33	300	3	1,000	500	54	37.8	54	5
34	300	3	1,000	500	54	37.8	54	8
35	300	2	1,000	500	54	37.8	54	7.2
36	300	3	Control	500	54	37.8	54	8
37	300	3	1,000	500	54	37.8	54	8

*Feed concentration for all the runs: 300 kg KCL/m^3, 30 kg NaCl/m^3, 10 kg $MgSO_4$/m^3.

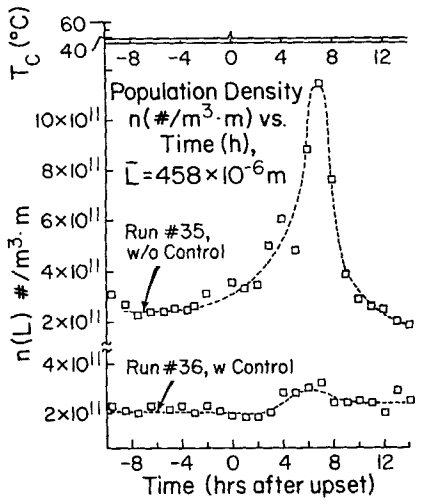

Figure 6. Population density vs. time at an average size of 458 × 10^{-6} m with and without control.

nuclei pulse (the disturbance), with or without control, as the disturbance grows down the particle size axis. Figures 6 and 7 plot population density vs. time for particle sizes of 458 × 10^{-6} m and 651 × 10^{-6} m with and without CSD control. Note that the population pulse is greatly attenuated in the run with CSD control (run 36). The vertical axis (population density) is repeated to allow superposition of the two runs. The temperature upset is also shown at the top of the figures.

The same information is plotted in Figures 8 and 9 as weight fraction on a given screen, ΔW_i vs. time for uncontrolled and controlled runs. Again, the large weight fraction disturbance that grows down the particle size axis is greatly attenuated when CSD control is implemented. However, it is apparent—as in Figure 9—that disturbance particles that escape the corrective action of the fines dissolver will ultimately show up as disturbances in the larger particle size ranges. Supposedly the weight fraction disturbance shown in the upper curve of Figure 9 would ultimately return to its original value, as no permanent changes in run conditions were made.

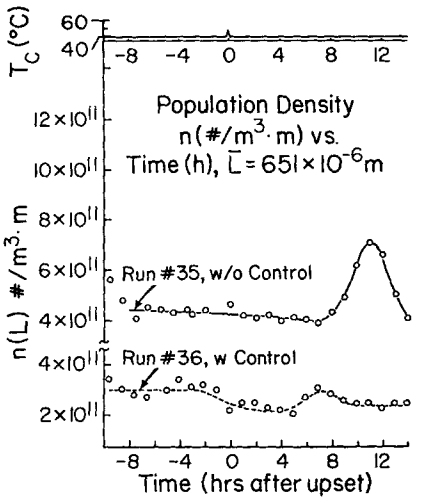

Figure 7. Population density vs. time at an average size fo 651 × 10^{-6} m with and without control.

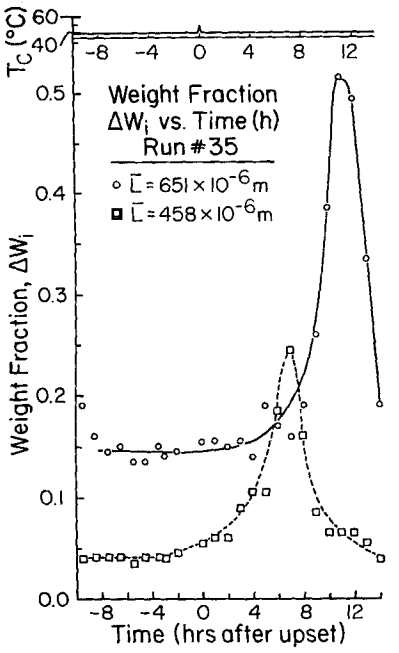

Figure 8. Weight fraction vs. time for average particle sizes of 458 × 10^{-6} m and 651 × 10^{-6} m.

Conclusions

Calculated PI_2 values indicate that RMS CSD fluctuations due to a nucleation upset were reduced by a factor of 3.5 with implementation of feedback control. Thus a significant improvement in CSD performance should be realized by application of this control technology. Nuclei density was estimated using both slurry density and particle size measurements from a well-conditioned fines stream. It was shown that only the former mea-

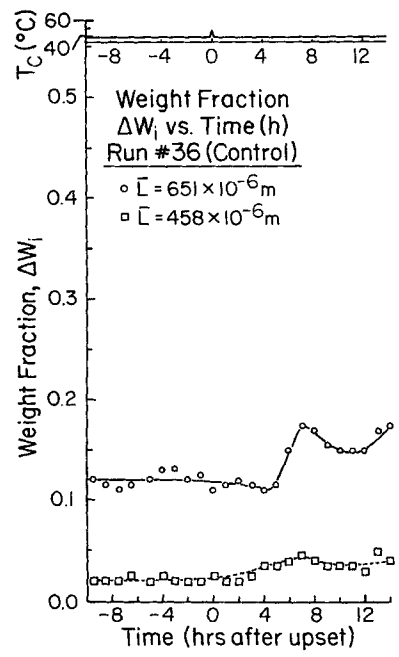

Figure 9. Weight fraction vs. time for average particle sizes of 458 × 10^{-6} m and 651 × 10^{-6} m.

surement (slurry density of fines) is needed to estimate nuclei density.

The addition of a recycle line to the fines dissolver stream enabled the flow Q_F to vary without introducing any upsets in the crystallizer, e.g., changing the cut size of the fines being removed. This permitted linear changes in fines destruction to be achieved via linear changes in the manipulated variable.

Simple proportional control of nuclei density in response to changes in fines removal rate was shown to be an effective way to minimize the effect of disturbances in nucleation rate on the product CSD.

Acknowledgment

This research was supported by National Science Foundation Grant No. CPE-8117753-02. The authors wish to thank Marco Scientific Co. (Sunnyvale, California) for use of the Cilas Granulometer 715 particle analyzer, and Syuji Tsuroka for development of the data analysis and control software.

Nomenclature

CW = cold water
F = flow meter
G = linear growth rate, length/time
H = heating tape
K_c = control gain
K_v = shape factor
L = linear size, length
M_T = slurry density, mass/volume of filtrate
M_{T_F}, M_{T_T} = slurry density of fines, mass/volume of filtrate
$n(L)$ = population density, number/volume of filtrate per length of particle
n^0 = nuclei density, number/volume of filtrate per length of particle
P = peristaltic pump
PI = performance index
Q_F = volumetric flow rate of fines destruction loop, volume/time
Q_i = volumetric feed rate, volume/time
Q_o = volumetric clear liquor overflow rate, volume/time
Q_P, Q_u = volumetric flow rate of product, volume/time
Q_R = volumetric flow rate of recycle, volume/time
ΔW_i = weight fraction of crystal product in sieve range i
T_c = crystallizer temperature, degrees
TC = temperature controller
ρ = crystal density, mass/volume
τ = residence time, Q/Q_p, time
τ_F = fines residence times, $V/(Q_F + Q_p + Q_o)$, time

Subscripts and superscripts

$()_F$ = fines stream
$()_i$ = ith size range
$()_t$ = value at sample period t
$\bar{()}$ = steady state or time-averaged value

Appendix

A representative nucleation disturbance is shown in Figure A1 as plots of fines slurry density in individual channels of the particle analyzer vs. time. Each channel corresponds to a given size range, as listed in Table A1. Figure A1 shows such a plot for run 36. Due to the initial rise in the crystallizer temperature caused by the shutdown of the cooling water valve, the amount of particles in all size ranges was reduced, i.e., small particles were dissolved in the crystallizer. Then as the cooling water valve reopened there was a burst of nuclei in the crystallizer and therefore a sudden increase in the number of small particles detected by the particle analyzer in all channels. Eventually the distribution returned to its previous form prior to the tempera-

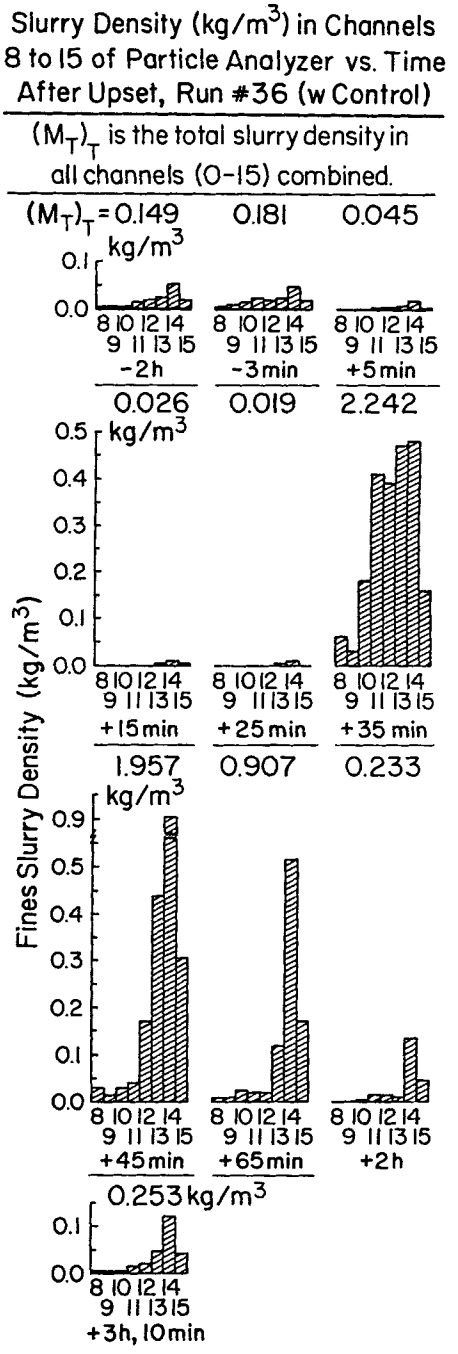

Figure A1. Variation of slurry density in channels 8–15 of particle analyzer vs. time after upset.

Table A1. Average Particle Size in Channels 8–15 of Particle Analyzer

Channel	$\bar{L}$ m × 10^{-6}
8	14
9	20
10	28
11	40
12	56
13	80
14	112
15	160

ture disturbance. The fines slurry density M_{T_F}, as measured by the Cilas instrument, is shown above each weight-channel histogram in Figure A1. Note that for run 36 the fines slurry concentration goes from practically nil (0.045 kg/m^3) to 2.24 kg/m^3 in the first 35 min after the temperature disturbance. Also note that the time $t = +35$ min corresponds to the maximum value of n^0 shown in Figure 2. Time zero is measured from the initial cutoff of cooling water; the 35 min time to the peak in fines density thus includes the crystallizer warmup and cool-down time.

Figure A2 shows similar histograms for a run without control implementation (run 33). Data were taken every 5 min, therefore allowing closer observation of the reaction of the particle analyzer to the nucleation upset. Again, due to the initial rise in the crystallizer temperature small particles were dissolved (see $t = +10$ min). Starting at $t = +15$ min there is a burst of new small particles moving down the size axis as a wave reaching larger sizes. Since no permanent changes in the operating conditions of the crystallizer were made, the distribution eventually returned to its steady state form. The difference in the times for peak M_T—and hence peak calculated n^0 values—between runs 33 and 36 is due solely to the different ΔT's and hence different times for warmup and cool-down of the crystallizer (see Table 3). Figures A3 and A4 show the average steady state distribu-

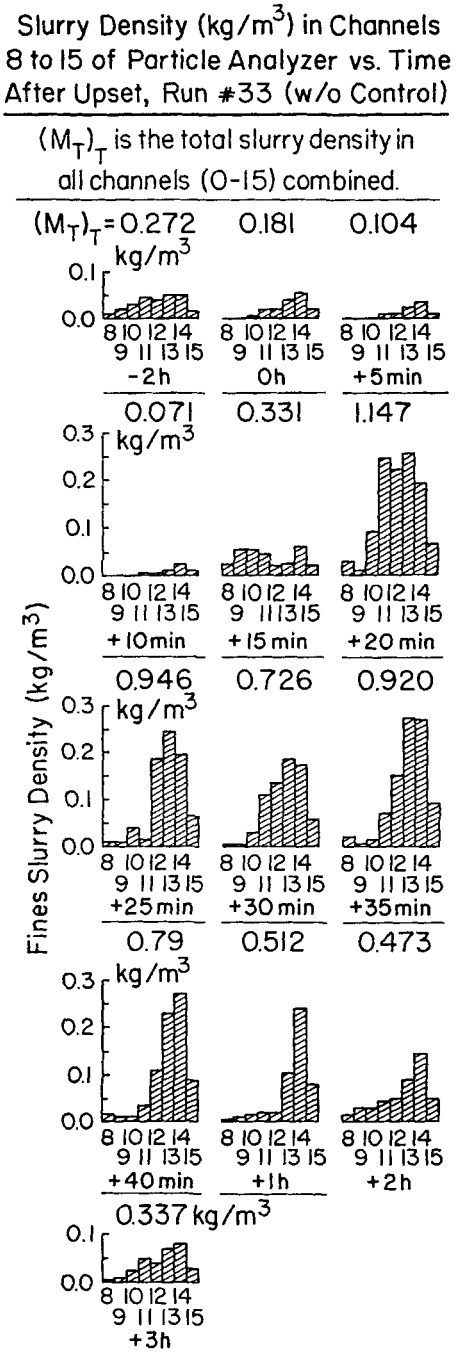

Figure A2. Variation of slurry density in channels 8–15 of particle analyzer vs. time.

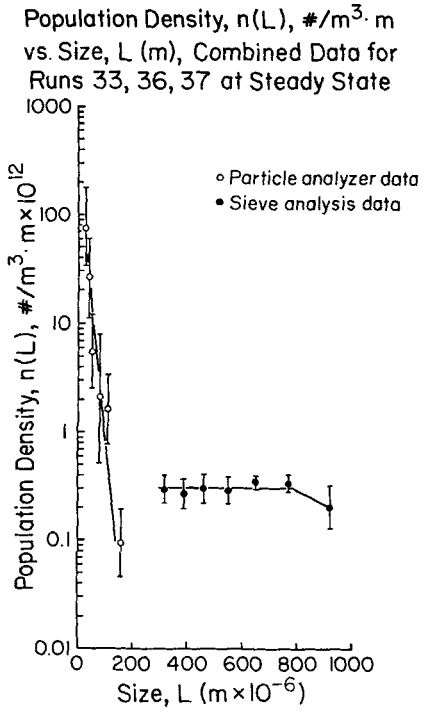

Figure A3. Population density vs. size for average steady state size distribution before upset.

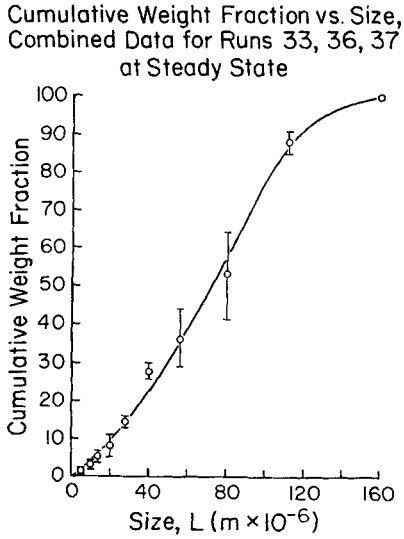

Figure A4. Average steady state distribution for all runs taken before any upsets.

tion of the crystallizer before any upsets expressed as population density and cumulative weight fractions. These steady state values did not vary appreciably among the various runs.

Literature cited

Beckman, J. R., and A. D. Randolph, "Crystal Size Distribution Dynamics in a Classified Crystallizer. II: Simulated Control of Crystal Size Distribution," *AIChE J.*, **23,** 510 (1977).

Epstein, M. A. F., and L. Sowul, "Phase Space Analysis of Limit Cycle Development in CMSMPR Crystallizers Using Three-Dimensional Computer Graphics," *AIChE Symp. Ser., No., 193,* **76,** 6 (1980).

Gupta, G., and D. C. Timm, "Predictive/Corrective Control for Continuous Crystallization," *AIChE Symp. Ser., No. 110,* **67,** 121 (1971).

Johnson, J. L., F. J. Schork, and A. S. Myerson, "Multivariable Control of an MSMPR Crystallizer," Paper 65b, AIChE Meet., Chicago (1985).

Lei, S. J., R. Shinnar, and S. Katz, "The Regulation of a Continuous Crytallizer with Fines Trap," *AIChE Symp. Ser., No., 110,* **67,** 129 (1971).

Randolph, A. D., and C. D. Low, "Some Attempts at CSD Control Utilizing On-line Measurement of Nucleation Rate," *Industrial Crystallization 8,* North-Holland (1982).

Randolph, A. D., E. T. White, and C. D. Low, "On-line Measurement of Fine-Crystal Response to Crystallizer Disturbances," *Ind. Eng. Chem. Process Des. Dev.*, **20,** 496 (1981).

Rousseau, R. W., and T. R. Howell, "Comparison of Simulated Crystal Size Distribution Control Systems Based on Nuclei Density and Supersaturation," *Ind. Eng. Chem. Process Des. Dev.*, **21,** 606 (1982).

Rovang, R., and A. D. Randolph, "On-line Particle Size Analysis in the Fines Loop of a KCl Crystallizer," *AIChE Symp. Ser., No., 193,* **76,** 18 (1980).

U.S. Patent No. 4,263,010, "Control Method and Apparatus for Crystallizer Process Control," (1981).

Manuscript received June 30, 1986, and revision received Oct. 6, 1986.